ELSEVIER

Journal of Molecular Catalysis A: Chemical 191 (2003) 123–134

JOURNAL OF MOLECULAR CATALYSIS A: CHEMICAL

www.elsevier.com/locate/molcata

Selective production of hydrogen by partial oxidation of methanol over Cu/Cr catalysts

Zhifei Wang, Jingyu Xi, Weiping Wang, Gongxuan Lu*

State Key Laboratory for Oxo Synthesis and Selective Oxidation, Lanzhou Institute of Chemical Physics, Chinese Academy of Sciences, Lanzhou 730000, PR China

Received 12 March 2002; accepted 25 June 2002

Abstract

Hydrogen production by partial oxidation of methanol ($CH_3OH + (1/2)O_2 \rightarrow 2H_2 + CO_2$) over a series of binary Cu/Cr catalysts and ternary Cu/Cr/M (M = Fe, Zn, Ce, etc.) catalysts prepared by co-precipitation method was studied. The results show that Cu60Cr40 catalyst exhibits high CH_3OH conversion and H_2 selectivity as compared with other binary catalysts and the introduction of Zn promoter not only helps to increase the activity of Cu60Cr40 catalyst but also improves the stability of the catalyst, the highest of the activity of the ternary Cu/Cr/Zn is obtained with a relative composition of Cu/Cr (6:4)/Zn (10%). The results obtained by XRD, H_2-TPR, BET methods and the measurement of the copper surface area by decomposition of N_2O reveal that catalyst performance for methanol conversion is dependent on the metallic copper surface area in the catalyst. Binary Cu/Cr catalysts containing less than 40% Cr enhance the dispersion of the metallic copper. Higher Cr content in the catalyst would lead to the formation of copper chromate that, on the contrary, decreases the surface area of the metallic copper. The stability results suggest that a rapid drop of activity of binary Cu60Cr40 catalyst during 100 h operation is due to the sintering of Cu species and the introduction of Zn helps to prevent Cu60Cr40 catalyst from being sintered to some extent.

Keywords: Methanol; Partial oxidation; Copper/chromium; Hydrogen

1. Introduction

Hydrogen is regarded as one of the most important energy carriers in the future because of its high energy efficiency and clean burning properties. It can be used directly as a fuel in internal combustion engines or indirectly to supply fuel cells. With the development of the technology of polymer electrolyte fuel cells (PEFCs), hydrogen fuel cell can exhibit thermal efficiency up to 35–40% [1]. But the wide use of hydrogen is limited because of the difficulties in its storage, transportation and distribution. The problems can be resolved by the on-board catalytic production of hydrogen from a suitable high energy density liquid fuel. Among all the liquid fuels, methanol is recognized as one of the hopeful candidates because of its ease of handling, low cost, and high-energy content as well as its commercialization as an important chemical feedstock [2].

Hydrogen can be obtained from methanol by different technologies such as steam reforming [3–5], decomposition [6–9], partial oxidation [10–15] or oxidative steam reforming [16–18]. Comparing with other technologies, there are some obvious advantages in the selective production of hydrogen by partial oxidation. Using oxygen (or air) instead of steam as the oxidant offers an exothermic reaction and higher

* Corresponding author. Fax: +86-931-8417088.
E-mail address: gxlu@ns.lzb.ac.cn (G. Lu).

1381-1169/02/$ – see front matter
PII: S1381-1169(02)00352-7

reaction rate which shortens the reaction time to reach the working temperature from the cold start-up and works under self-thermo-balanced conditions.

Previous studies on partial oxidation of methanol to produce hydrogen largely concentrated on Cu/Zn/Al [12,15] or ZnO- and ZrO-supported Pd catalysts [13,14]. However, over Cu/Cr catalysts, only methanol decomposition was studied [7–9], partial oxidation of methanol was less studied. The aim of this work is to examine hydrogen generation over Cu/Cr catalysts via partial oxidation of methanol. To learn about the relationships between the characteristics of the catalyst, such as structure, surface chemical states, and catalyst performance in methanol partial oxidation reaction is of particular interest. In addition, the effect of the promoters (such as Fe, Zn, Ce) on the performance of Cu/Cr (6:4) catalyst will be studied as well.

2. Experimental

2.1. Preparation of catalysts

Cu/M/Cr (M = Zn, Ce, Fe, etc.) catalysts were prepared using the co-precipitation method. Catalyst precursors were prepared by adding an aqueous solution of some of the metal salts, i.e. $Cu(NO_3)_2{\cdot}3H_2O$, $Cr(NO_3)_3{\cdot}9H_2O$, $M(NO_3)_x{\cdot}yH_2O$, depending on the required catalyst components, to a vigorously stirred solution of Na_2CO_3 (1.8 M) at room temperature. For example, for Cu60Cr40 catalyst, the initial concentrations of copper nitrate and chromic nitrate were 0.6 and 0.4 M, respectively. And pH value of the solution was maintained at 10 for 2 h. The resulted precipitate was filtered and washed with distilled water until pH reached 7, then dried in air at 120 °C overnight. Finally the co-precipitated catalyst precursors were calcined in air at 350 °C for 3 h and crashed to 40–60 mesh.

2.2. Study on the reaction

The calcined catalysts were reduced in situ by 10% H_2 in N_2 stream (flow rate 50 ml/min) at 300 °C for 2 h before reaction. Partial oxidation reaction was carried out in a fixed-bed continuous flow quartz reactor (∅ 4 mm). Typically, 200 mg of catalyst was used each time and mixed with quartz chips. Methanol was supplied using N_2 and air as carriers in a set of jacketed saturator which was heated by an external heating bath. The total flow rate was kept at 24 ml/min with the pressure of the reaction at 1 atm. Gas phase effluents were analyzed by two on-line chromatographs. One was equipped with a 13× molecular sieve column and a thermal-conductivity detector (TCD), the other, with a porapak Q column and a flame ionization detector (FID).

2.3. Characterization

2.3.1. X-ray diffraction (XRD)

Powder XRD patterns of the samples were recorded on a Rigaka b/max-RB Diffractometer with a nickel filtrated Cu Kα radiation, 2θ angles from 10 to 80° were recorded at a scanning speed of 2°/min The samples after reaction were transferred under a N_2 atmosphere to the diffractometer.

2.3.2. Temperature-programmed reduction (TPR)

The TPR of the catalyst was performed at atmospheric pressure in a conventional flow system built in our laboratory at a linearly programmed rate of 10 °C/min from 20 to 550 °C (5% H_2 in Ar stream, flow rate 50 ml/min). About 0.1 g of sample was used for each run. The amount of the consumed H_2 was determined by a TCD. Before each measurement, the samples were purged with dry air at 400 °C for 1 h.

2.3.3. BET and Cu^0 surface area

BET surface area measurements were performed by the nitrogen adsorption isotherms using Micromeritics ASAP2010 Adsorption Instrument. The surface area of Cu^0 was determined by N_2O titration method according to the following equation:

$$N_2O + 2Cu(s) = Cu_2O + N_2$$

The measurements were carried out using 200 mg of catalyst in an "U" shape quartz reactor (∅ 4 mm). Before measurement, the catalyst was reduced by a 10% H_2 (He balanced) at 200 °C for 30 min, at 250 °C for another 30 min, and by pure H_2 at 250 °C for the third 30 min. Then, the pre-reduced sample was purged by pure He at 250 °C for 60 min and cooled to 40 °C in He. N_2O was fed in pulses (200 μl each) into a carrier gas stream of helium (with a flow rate of 50 ml/min). The released N_2 was determined on a

quadrupole mass spectrometer (Ametek Instruments, Dycor system 1000) [19].

2.3.4. X-ray photoelectron spectrometric (XPS)

XPS analyses were performed in order to verify the species on the surface of the used catalysts. The used catalysts were kept in nitrogen atmosphere during the transfer to the XPS measurement apparatus. X-ray photoelectron spectra were acquired on a VG ESCALAB 210 Electron Spectrometer, equipped with a hemispherical electron analyzer and a Mg Kα X-ray source ($h\nu = 1253.6$ eV). The XPS data were calibrated by the binding energy (BE) of C1s peak at 284.6 eV. The spectra were analyzed in terms of $Cu2p_{3/2}$ bind energy and $Cu2p_{3/2L3M4,5M4,5}$ Auger levels.

3. Results

3.1. Catalyst characterization

The BET and metallic Cu^0 surface areas for Cu/Cr catalysts after pre-reduction are shown in Table 1. Comparing the BET and metallic Cu^0 surface areas of pure metallic Cu catalyst with that of Cu/Cr catalysts, it is found that generally, the introduction of chromium increases the surface area of Cu^0, but when the chromium content is over 80%, the BET surface areas of Cu/Cr catalysts are less than that of pure metallic Cu catalyst. BET and metallic Cu^0 surface areas of Cu/Cr catalysts ascend with the increase of chromium content and reach maxima (53.65 and 17.98 m^2/g, respectively) for Cu60Cr40 catalyst and the surface areas decrease at the increase of chromium concentration.

XRD patterns of Cu/Cr catalysts after reaction are shown in Fig. 1. It can be seen that the catalysts change with the increase of chromium content. When the chromium content is below 40%, Cu species in the catalysts mainly exits as Cu_2O and Cu^0, and no XRD peak of species containing chromium appears, which suggests that the species containing chromium is highly dispersed and exists in an amorphous state. It is found that the FWHMs of the XRD peaks of Cu_2O and Cu^0 species in Cu60Cr40 catalyst are broader than that in Cu80Cr20 catalyst, which suggests that the mean particle sizes of Cu_2O and Cu^0 species become smaller with the increase of chromium content. Combining this with BET and Cu^0 surface area results, we concluded that when the chromium content is 40%, BET and Cu^0 surface areas are at maxima, while an appropriate introduction of chromium improves the dispersion of copper and increases the BET and Cu^0 surface areas. On the other hand, when the chromium content is above 40%, with the increase of chromium content, new peaks appear in the XRD patterns, for Cu40Cr60 catalyst, the peak at 18° can be assigned to $CuCrO_4{\cdot}2CuO$ and the peak at 36.3° can be attributed to Cu_2O and $CuCrO_4{\cdot}2CuO$ species. For Cu20Cr80 catalyst, the peaks at 24.3, 33.4, 35.9° can be assigned to $CuCrO_4$ species. No peaks at 41.2, 54.5, 63, and 64.7° can be found. From the above analysis, it is believed that with chromium content up to 40% the introduction of chromium helps to improve the dispersion of Cu^0 species and to increase the Cu^0 surface area, while further increase of chromium content leads to the production of copper chromates, such as $CuCrO_4{\cdot}2CuO$ and $CuCrO_4$ which, on the contrary, decreases the Cu^0 surface area. In addition, it can be inferred that the active site of Cu/Cr catalysts is related to the Cu^0 species.

Table 1
BET and Cu^0 surface area of the reduced binary Cu/Cr catalysts

Catalyst	BET (m^2/g)	Cu^0 (m^2/g)
Cu	14.87	1.84
Cu20Cr80	8.01	5.97
Cu40Cr60	41.79	4.78
Cu60Cr40	53.65	17.98
Cu80Cr20	41.79	16.18

Fig. 2 shows the patterns of TPR of the calcined Cu/Cr catalysts. Patterns a–e represent the TPR patterns of pure copper oxide, Cu80Cr20, Cu60Cr40, Cu40Cr60 and Cu20Cr80, respectively. It can be seen that the symmetrical reduction peak of pure copper oxide at 287 °C (CuO to Cu^0) means that only one species is reduced. When Cr is introduced into the catalysts, the TPR patterns become broader and asymmetrical and can be divided into two peaks, which suggests that at least two species are reduced (see patterns b–d). Because the temperature of the first peaks in patterns b–d is similar to the temperature of the pure copper oxide reduction peak, it can be concluded that this peak represents the reduction of CuO in the catalyst. The temperature of the second reduction peak

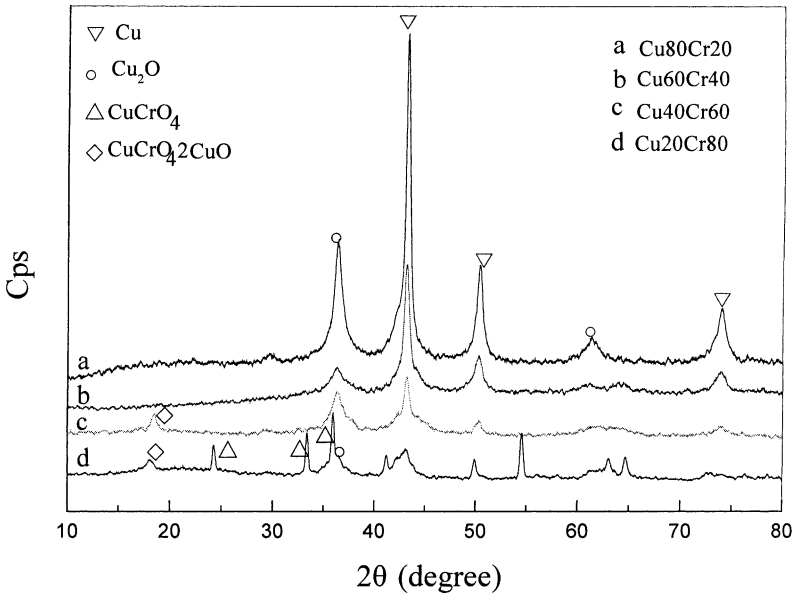

Fig. 1. XRD patterns of binary Cu/Cr catalysts after the reaction at 473 K, $O_2/CH_3OH = 0.5$: pattern a, Cu80Cr20; pattern b, Cu60Cr40; pattern c, Cu40Cr60; pattern d, Cu20Cr80.

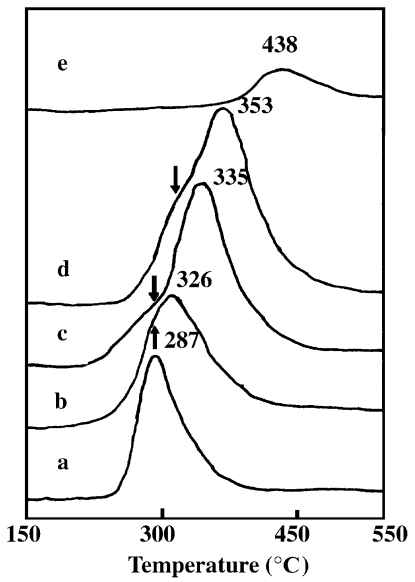

Fig. 2. H_2-TPR profiles of binary Cu/Cr catalysts: pattern a, Cu; pattern b, Cu80Cr20; pattern c, Cu60Cr40; pattern d, Cu40Cr60; pattern e, Cu20Cr80.

is affected by the Cr concentration. With the increase of chromium content, this peak shifts to higher temperature. Based on the XRD patterns, this reduction peak can be attributed to the reduction of high valence copper chromate to low valence one [20]. The main peak of the pattern e at 438 °C is the typical reduction peak of copper chromate species and the hydrogen consumption corresponding to the reduction of high valence copper chromate to low valence one is small, apparently only part of the copper is being reduced. So it can be concluded that with the increase of chromium content the reduction temperature shifts to higher temperature and excess of chromium not only decreases Cu^0 surface area but also increases the reduction temperature. As we know, higher reduction temperature is not favorable to improve the activity of the catalyst.

The XPS patterns of Cu/Cr catalysts after reaction are shown in Fig. 3. Patterns a and b represent Cu60Cr40 and Cu20Cr80 catalysts, respectively. The XPS BEs and the characteristic core levels of Cu in different catalysts are listed in Table 2. Comparing these data with the standard BEs and the modified Auger parameter, it can be concluded that for patterns a and b, the strong $Cu2p_{3/2}$ peaks (ca. 932.5, and 1851.09 eV)

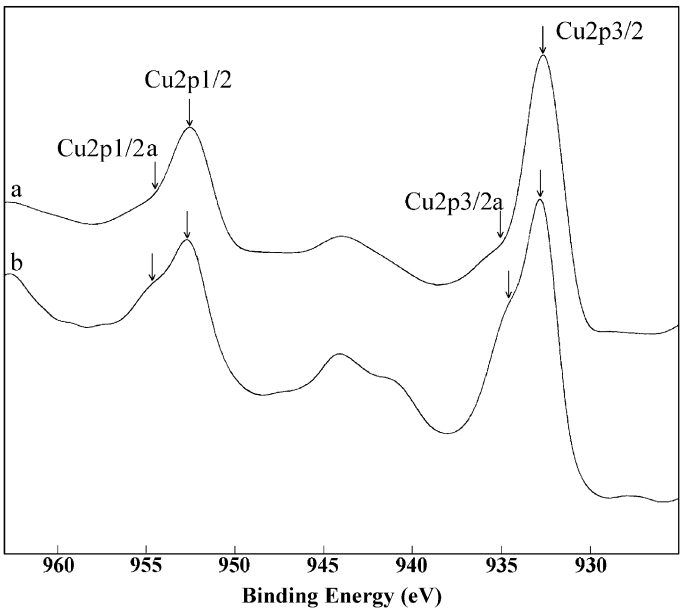

Fig. 3. $Cu2p_{3/2}$ core level spectra of catalysts: pattern a, Cu60Cr40; and pattern b, Cu20Cr80 after reaction using feed ratio O_2/CH_3OH of 0.5 at 473 K.

and shoulder peaks (ca. 935.7 and 1849.15 eV) can be assigned to Cu^0 and Cu^{2+} species, respectively. The content of Cu^{2+} in Cu20Cr80 catalyst is higher than that of Cu60Cr40 catalyst. These results agree with the XRD results, which indicate that Cu20Cr80 catalyst is mainly consisted of copper chromate and Cu species exists as Cu^{2+}. From the above analysis, it can be inferred that Cu^0 and Cu^{2+} species are present during reaction. Since it has been reported that Cu^{2+} species is not the active site of Cu based catalyst for methanol partial oxidation reaction [12], we suggest that the active sites of catalyst are related to Cu^0 species. In addition, the content of Cu^0 species in Cu60Cr40 catalyst is higher than that of Cu20Cr80 catalyst, which is consistent with the catalyst activity.

Table 2
XPS data of the catalysts

Sample	Cu $2p_{3/2}$ position (eV)	Cu LMM Auger KE (eV)	Auger parameter + photon energy (eV)
Cu60Cr40	935.29	337.02	1849.15
	932.57	335.08	1851.09
Cu20Cr80	934.57		1849.55
	932.65	336.70	1851.47

3.2. Catalytic activity of binary Cu/Cr systems

In the following measurements, besides the major products of the reaction (H_2, CO, CO_2, and H_2O), the trace amounts of the by-products, such as formaldehyde (HCHO), methyl formate ($HCOOCH_3$), and dimethyl ether (CH_3OCH_3), have been detected when the O_2/CH_3OH molar ratio is low (see Table 3), and O_2 conversion reaches 100%. When the O_2/CH_3OH molar ratio is 0.5, only major products are detected, in addition, trace amounts of O_2 are found in the product. NO methane is detected in any of these measurements.

3.2.1. Effect of chromium content

Fig. 4 shows the effects of chromium content on methanol conversion and H_2, CO, CO_2 selectivity under O_2/CH_3OH molar ratio 0.5 at 473 K. It is observed that methanol conversion increases with the increase of chromium content and reaches a maximum when Cr content is about 40% for Cu60Cr40 catalyst, then decreases when Cr content is higher than 40%. The

Table 3
Methanol partial oxidation with various O_2/CH_3OH molar ratios

O_2/CH_3OH	Initial selectivity (%)[a]						Balance			X_{CH_3OH} after 2 h (%)
	CO	CO_2	MF × 2	DME × 2	FA	H_2O	H_2	H/4C	O/C	
0.1	18.2	64.5	0.96	4.7	6.1	0.2	77.6	0.99	1	33.6
0.2	12.4	76.9	0.86	3.2	2.6	5.9	80.2	1	0.97	46.2
0.3	7.5	82.3	0.73	2.8	3.1	12.6	74.3	0.99	0.95	55.4
0.4	11.4	86.2	0.2	–	–	19.1	80.3	0.99	1.01	78.5
0.5	12.2	87.8	–	–	–	31.9	68.1	1	–	86.5

Reaction temperature 473 K.
[a] MF: methyl formate; DME: dimethyl ether; FA: formaldehyde.

relationship between methanol partial oxidation and copper metal surface area can also be clearly observed. The catalyst Cu60Cr40 having high metallic copper area is the most active catalyst for partial oxidation of methanol. In addition, for H_2, CO_2 selectivities, it can be seen that H_2 selectivity drops rapidly and CO_2 selectivity increases when chromium content reaches 80%. The XRD results indicate that in this catalyst copper exists mainly as $CuCrO_4{\cdot}2CuO$, $CuCrO_4$ and other copper chromium species, which suggests that the presence of Cu^{2+} species favors the methanol deep oxidation to CO_2 and H_2O. So it can be concluded that the activity of catalyst is related to copper surface area and Cu^{2+} species favors methanol deep oxidation to CO_2 and H_2O.

3.2.2. *Effect of O_2/CH_3OH molar ratio*

The effect of O_2/CH_3OH molar ratio on the activity of catalyst Cu60Cr40 at 473 K is listed in Table 3. Generally, the mass balance errors are less than 5%. As indicated in Table 3, when the O_2/CH_3OH ratio increases from 0.1 to 0.5, i.e. the amount of oxygen increases, methanol conversion increases obviously from 33.6 to 86.5 which suggests that the introduction of O_2 is helpful to enhance the activity of catalyst. According to Fisher and Bell [24], who studied methanol decomposition on Cu/SiO_2, ZrO_2/SiO_2, and $Cu/SiO_2/ZrO_2$, the pre-absorbed oxygen on the catalyst surface is favorable to the chemisorption of methanol. In addition, Herman et al. [25] found that the activity of copper–zinc catalysts was due to a

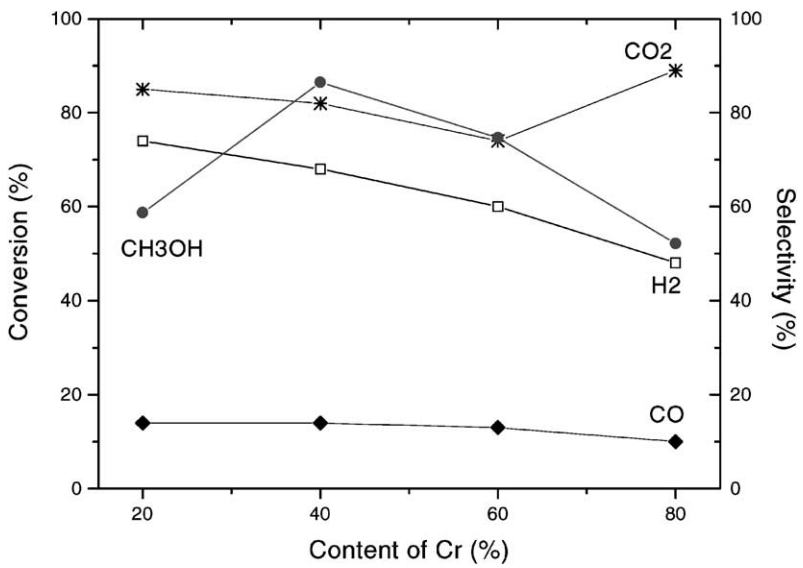

Fig. 4. Effect of Cr content on the performance of binary Cu/Cr catalysts using feed ratios O_2/CH_3OH of 0.5 at 473 K.

partially oxidized copper surface Cu(I). So the introduction of oxygen leads to the enhancement of the oxidative atmosphere of the reactant, which is helpful to the redox reactions of Cu^0.

With the increase of oxygen introduced, the CO selectivity decreases and reaches the minimum value when the O_2/CH_3OH molar ratio is 0.3, and then increases. The reason for this is that methanol decomposition occurs during the reaction besides methanol partial oxidation and the proportion between these two changes with the increase of O_2. When the amount of oxygen is below 0.3, the content of methanol decomposition decreases with the increase of oxygen. And when the O_2/CH_3OH molar ratio reaches 0.5, the high exothermicity of methanol partial oxidation enhances the process of methanol decomposition reaction, so CO selectivity is high when O_2/CH_3OH ratios in the feed is close to the stoichiometry of methanol partial oxidation. The simultaneous increase of CO_2 and H_2O selectivity with the increase of O_2/CH_3OH molar ratio indicates that the reaction $CO + (1/2)O_2 \rightarrow CO_2$ is involved and WGS reaction ($CO + H_2O \rightarrow CO_2 + H_2$) does not occur. This can also be confirmed by the value of ($P_{H_2} \times P_{CO_2}/P_{H_2O} \times P_{CO}$) since it is lower than the equilibrium constant of WGS reaction ($K = P_{H_2} \times P_{CO_2}/P_{H_2O} \times P_{CO} = 142.8$ at 498 K) [12]. For H_2 selectivity, this effect is not evident with the introduction of O_2 except for O_2/CH_3OH ratios of 0.5. Comparing with the CH_3OH conversion and H_2O, CO selectivity, it can concluded that H_2 can be oxidized to water ($H_2 + (1/2)O_2 \rightarrow H_2O$) when the content of O_2 is high.

In addition to the major products of the reaction (H_2, CO, CO_2, and H_2O), trace amounts of by-products, such as HCHO, CH_3OCH_3, and $HCOOCH_3$, have been detected when the O_2/CH_3OH molar ratio is low. Cheng [7] found that the production of dimethyl ether could be correlated with the composition of Cr in a variety of Cu based catalysts and only a small amount of dimethyl ether had been found in the absence of Cr during methanol decomposition. These results further confirm the above assumptions that methanol decomposition is involved in the reaction. In addition, according to the literature [26,27], HCHO can be formed in the oxidation of methanol. Thus, main reactions occurred during the reaction can be represented by the following equations [7,26,27]:

$$CH_3OH \rightarrow CO + 2H_2 \quad (2CH_3OH \rightarrow HCOOCH_3 + 2H_2 \rightarrow CH_3OH + CO + H_2 \quad \text{or} \quad 2CH_3OH \rightarrow CH_3OCH_3 + H_2)$$

$$CH_3OH + \tfrac{3}{2}O_2 \rightarrow HCHO + \tfrac{1}{2}H_2 + \tfrac{1}{2}H_2O$$

$$CO + \tfrac{1}{2}O_2 \rightarrow CO_2$$

$$H_2 + \tfrac{1}{2}O_2 \rightarrow H_2O$$

$$CH_3OH + \tfrac{1}{2}O_2 \rightarrow CO_2 + 2H_2$$

The participation of the above reactions is dependent on the variance of O_2/CH_3OH ratios.

3.2.3. *Effect of temperature*

The effect of reaction temperature on the main products of the reaction over catalyst Cu60Cr40 is listed in Table 4. At O_2/CH_3OH ratios of 0.3, it can be seen that with the increase of reaction temperature methanol conversion increases from 55.4% at 473 K to 88.3% at 523 K, at the same time CO selectivity increases from 7.5 to 13.5% but there is less effect on H_2 selectivity. As mentioned above, methanol decomposition is involved in the reaction, so the increase of

Table 4
Methanol partial oxidation with the different O_2/CH_3OH ratios and reaction temperatures

O_2/CH_3OH	Reaction temperature (K)	CH_3OH conversion (%)	CO selectivity (%)	CO_2 selectivity (%)	H_2 selectivity (%)
0.3	473	55.4	7.5	82.3	77.6
	493	65.1	9.8	84.2	80.6
	523	88.3	13.5	83.2	82.3
0.5	473	86.5	12.2	87.8	68.1
	493	90.3	14.3	85.7	67.2
	523	93.5	13.2	86.8	69.2

temperature is favorable to the progress of methanol decomposition and the content of CO in the products increases. At O_2/CH_3OH ratios of 0.5, it can be seen that methanol conversion increases with the increase of the reaction temperature and there is less effect to H_2, CO, and CO_2 selectivities. The above results indicate that the influence of temperature on the reaction is greater at the low O_2/CH_3OH ratio than that at the high O_2/CH_3OH ratio. In the former case, methanol decomposition is easy to proceed at high temperature.

3.3. Effect of promoter

The effect of the different promoters in Cu60Cr40 catalyst for partial oxidation of methanol was studied and the results of reaction at 473 K, O_2/CH_3OH = 0.5 are shown in Table 5. M (M = Ce, Co, Ni, etc.) content is kept at 10% and the molar ratio of Cu/Cr is kept at 6:4. It can be seen that the introduction of Zn improves the MeOH conversion from 86.5% for Cu60Cr40 to 96% for Cu/Cr/Zn (10%), and has little effect on the product selectivity. The introduction of Mg, Zr, Fe, Al obviously decreases MeOH conversion and H_2 selectivity. On the other hand, the presence of Co, Ce, Ni has little effect on MeOH conversion, but decreases H_2 selectivity. The introduction of Ni obviously improves the CO selectivity from 14% for Cu60Cr40 to 31.4% for Cu/Cr/Ni (10%), which means that the presence of Ni favors methanol decomposition in the reaction. It is reported that the introduction of Zn is favorable to improve the dispersion of Cu^0 species [7]. As mentioned above, the activity of the catalysts is related to Cu^0 species. So the introduction of Zn is favorable to improve the performance of Cu60Cr40 catalyst.

The effect of Zn content on the performance of ternary Cu/Zn/Cr catalysts is shown in Fig. 5. It can be seen that with the increase of the amount of introduced Zn, the MeOH conversion first increases and reaches a maximum when Zn content reaches 10%, and then decreases. The same trend can be found for H_2 selectivity. So it can be found that the activity maximum of the ternary Cu/Cr/Zn catalysts is obtained for a relative composition of Cu/Cr (6:4)/Zn (10%).

3.4. Catalysts stability

The stability of the two catalysts, Cu60Cr40 and Cu/Zn (6:4)/Cr (10%) was studied in a period of 100 h at 473 K with the O_2/CH_3OH ratio of 0.5. The results are displayed in Fig. 6. It can be founded that the binary catalyst Cu60Cr40 deactivates at the beginning and the MeOH conversion drops from 86.5% to an approximate 40% after 30 h operation, and then keeps almost constant in another 70 h operation. Similarly, the ternary catalyst Cu/Zn (6:4)/Cr (10%) deactivates from the beginning, but the extent of activity drop is smaller than that for the binary catalyst Cu60Cr40. The MeOH conversion only drops from 96% to an approximate 80% after 30 h operation and keeps nearly constant in another 10 h, then it drops from 80 to 60% in the further operation. From the above analysis, it can be concluded that the introduction of Zn not only increases the performance of binary Cu60Cr40 but also improves its stability.

Table 5
Methanol partial oxidation over different Cu/Cr/M catalysts

Catalyst[a]	MeOH conversion (%)	H_2 selectivity (%)	CO_2 selectivity (%)	CO selectivity (%)
Cu/Cr/Co (10%)	84.2	60	85.8	14.2
Cu/Cr/Ce (10%)	90.2	58.2	82.5	17.5
Cu/Cr/Ni (10%)	88.6	53.8	68.6	31.4
Cu/Cr/Mg (10%)	70	57.1	82.7	17.3
Cu/Cr/Zr (10%)	79.1	57.1	84.7	15.3
Cu/Cr/Zn (10%)	96.1	62.5	87.5	12.5
Cu/Cr/Fe (10%)	61.5	44.4	89.9	10.1
Cu/Cr/Al (10%)	77	45.4	81.7	18.1
Cu/Cr	86.5	68.1	87.8	12.2

Reaction temperature: 473 K.
[a] Cu/Cr molar ratio in the above catalysts are 6:4.

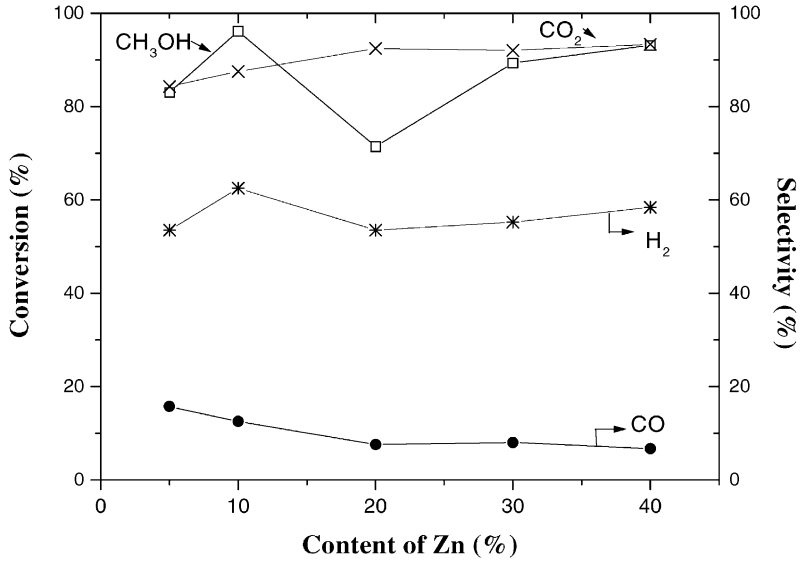

Fig. 5. Effect of Zn content on the performance of ternary Cu/Zn/Cr catalysts using feed ratios O_2/CH_3OH of 0.5 at 473 K.

3.5. XRD characteristics of Cu60Cr40 and Cu/Cr/Zn (10%) catalysts after reaction

The XRD patterns of Cu60Cr40 catalyst after different reaction times are shown in Fig. 7, for patterns a and b the reaction times are 100 and 1 h, respectively. It can be seen that the catalysts after reaction consist of Cu^0 and Cu_2O species independent of the reaction time and the intensities of Cu_2O and Cu^0 peaks in pattern a are stronger than that in pattern b, which suggests that the extent of crystallization of Cu_2O and Cu^0 species in pattern a is higher than that in pattern b, that is, the crystallinity of the catalyst increases during the 100 h operation. As mentioned above, the activity

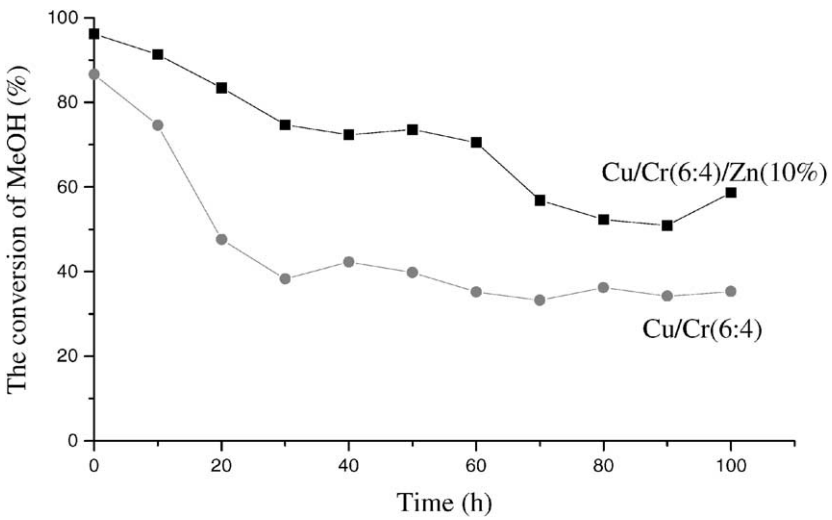

Fig. 6. Time-on-stream experiments over binary Cu60Cr40 catalyst and ternary Cu/Cr (6:4)/Zn (10%) catalyst using feed ratios O_2/CH_3OH of 0.5 at 473 K.

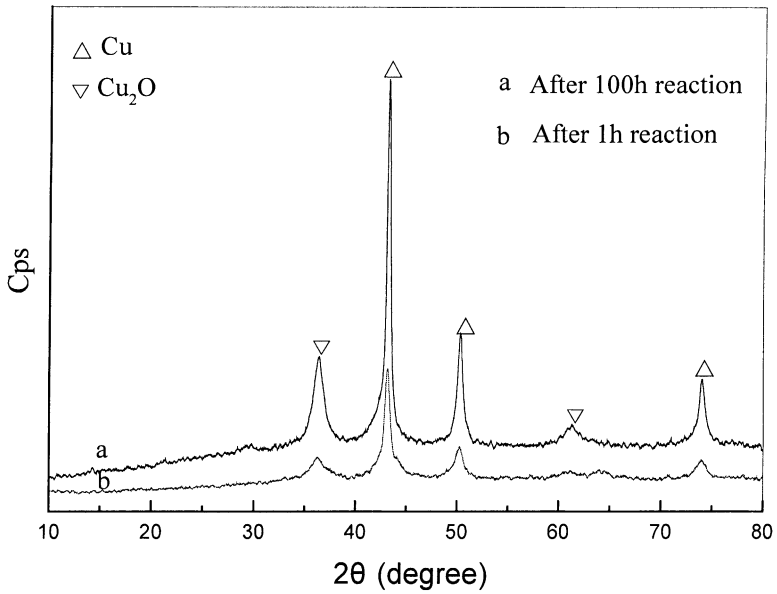

Fig. 7. XRD patterns of binary Cu60Cr40 catalyst: pattern a, after 100 h reaction; and pattern b, after 1 h reaction using feed ratios O_2/CH_3OH of 0.5 at 473 K.

of catalyst drops obviously after 100 h operation. So it can be concluded that sintering of copper is one of the causes of the activity drop and high crystallinity of Cu_2O and Cu^0 is not favorable to the catalystic activity.

The same phenomenon can be seen in Fig. 8, which shows the XRD patterns of Cu/Cr (6:4)/Zn (10%) catalyst after 100 and 1 h (patterns a and b), respectively. The extent of drops in the peak intensities of Cu_2O

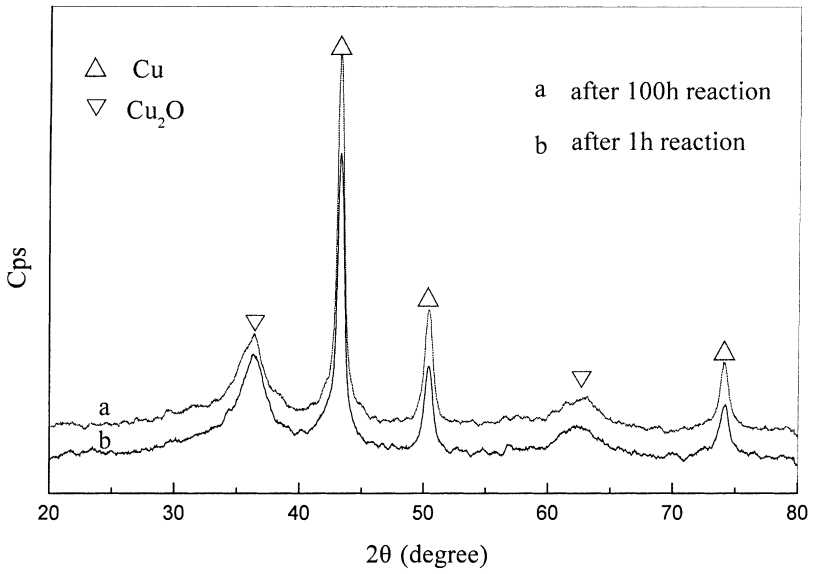

Fig. 8. XRD patterns of ternary Cu/Cr (6:4)/Zn (10%) catalyst: pattern a, after 100 h reaction; and pattern b, after 1 h reaction using feed ratios O_2/CH_3OH of 0.5 at 473 K.

and Cu^0 species in Cu/Cr (6:4)/Zn (10%) catalyst is smaller than that in Cu60Cr40 catalyst. This suggests that the structure change in the latter structure is larger than that in the former. So it can be concluded that the introduction of Zn is favorable to improve the stability of Cu60Cr40 catalyst and prevent it from sintering.

4. Discussion

In the series of Cu/Cr catalysts, Cu60Cr40 catalyst shows the highest metallic copper surface area (17.98 m^2/g). This catalyst also showed the highest activity for the methanol partial oxidation. The remarkable dependence of the catalyst activity on the copper surface area suggests that the metallic copper on the surface is necessary for the active catalyst of methanol partial oxidation to hydrogen (see the results in Table 1).

XPS results show that copper on the surface of catalyst after reaction mainly exists as Cu^0 and Cu^{2+} in binary Cu/Cr catalysts and Cu^+ species is not found. As we know that Cu^{2+} species is not the active site and the presence of Cu^{2+} species favors methanol deep oxidation to CO_2 and H_2O. So it can be suggested that the active site must be related to Cu^0 species. But here we cannot exclude the possibility of Cu^+ species being the active site, because XRD studies show that binary Cu/Cr and ternary Cu/Cr (6:4)/Zn (10%) catalysts contain crystalline Cu and Cu_2O after the reaction.

The formation of Cu^+ by re-oxidation from Cu^0 species in air is possible, especially for highly dispersed Cu^0 species, which can consequently lead to the coexistence of Cu^0 and Cu^+ in the used Cu/Cr catalyst [21,22]. According to [23], the Cu^+ species is helpful to adsorb and dissociate CH_3OH via formation of Cu^+–carbonyl species [Cu^+–CO], and hydrogen atoms formed in the dissociation of CH_3OH shift to Cu^0 and form hydrogen molecule which desorbed from the Cu^0 surface. In addition, the results of the promoters, such as Zn, Ce, Co, Fe, etc. show that the introduction of Zn promoter is favorable not only to increase the activity but also to improve the stability of Cu/Cr catalysts and prevent the Cu species from sintering. Alejo et al. [12] reported that the introduction of Zn is helpful to increase the dispersion of Cu^0 and Cu^+ species and improve the stability of Cu^+ species. So it can be speculated that the active centers might be connected with the Cu^0 and Cu^+ in Cu/Cr catalyst and further work is still needed to identify the nature of the active centers in Cu/Cr catalysts for the partial oxidation of methanol to hydrogen.

5. Conclusions

(1) The introduction of chromium up to 40% increases the dispersion of copper and the Cu^0 surface area of Cu/Cr catalysts, and higher Cr content leads to the production of copper chromate that, on the contrary, decreases BET and Cu^0 surface areas.
(2) Of all binary Cu/Cr catalysts, Cu60Cr40 catalyst exhibits the highest activity for hydrogen generated from methanol, so high BET and Cu^0 surface area is favorable to improve the activity of binary Cu/Cr catalysts. The active site is related to the Cu^0 species, and the Cu^{2+} species favors the methanol deep oxidation to CO_2 and H_2O.
(3) The introduction of Zn as a promoter to the binary Cu/Cr catalysts is favorable not only to increase the activity but also to improve its stability. The highest activity of the ternary Cu/Cr/Zn catalysts is obtained for a relative composition of Cu/Cr (6:4)/Zn (10%).
(4) The XRD results of Cu60Cr40 and Cu/Cr (6:4)/Zn (10%) catalysts after deactivation show that the sintering of Cu^0 is one of the main reasons of deactivation and the introduction of Zn is favorable to prevent Cu60Cr40 catalyst from sintering to some extent.

Acknowledgements

The authors are grateful to the 973 project of China (G20000264).

References

[1] B. Lindner, K. Sjomstrom, Fuel 63 (1984) 1485.
[2] W. Cheng, H.H. Kung, Methanol Production and Use, Marcel Dekker, New York, 1994.
[3] R.O. Idem, N.N. Bakhshi, Ind. Eng. Chem. Res. 34 (1995) 1548.

[4] R.O. Idem, N.N. Bakhshi, Can. J. Chem. Eng. 74 (1996) 288–300.
[5] B.E. Goodby, J.E. Pemberton, Appl. Spectrosc. 42 (1988) 754.
[6] W.-J. Shen Yasuyuki Matsumura, Phys. Chem. Chem. Phys. 2 (2000) 1519–1522.
[7] W.-H. Cheng, Appl. Catal. A: Gen. 130 (1995) 13–30.
[8] W.-H. Cheng, Appl. Catal. B: Environ. 7 (1995) 127–136.
[9] W.-H. Cheng, C.-Y. Shiau, T.H. Liu, et al., Appl. Catal. B: Environ. 18 (1998) 63–70.
[10] T.-J. Huang, S.-W. Wang, Appl. Catal. 24 (1986) 287–297.
[11] T.J. Huang, S.L. Chren, Appl. Catal. 24 (1986) 287–297.
[12] L. Alejo, R. Lago, M.A. Pena, et al., Appl. Catal. A: Gen. 162 (1997) 281–297.
[13] M.L. Cubeiro, J.L.G. Fierro, Appl. Catal. A: Gen. 168 (1998) 307–322.
[14] M.L. Cubeiro, J.L.G. Fierro, J. Catal. 179 (1998) 150–162.
[15] S. Velu, K. Suzuki, T. Osaki, Catal. Lett. 62 (1999) 159–167.
[16] S. Velu, K. Suzuki, M. Okazaki, J. Catal. 194, 373–384.
[17] T.L. Reits, S. Ahmed, M. Krumpelt, et al., J. Mol. Catal. A: Chem. 162 (2000) 275.
[18] S. Muricia-Mascaros, R.M. Navarro, L. Gomez-Sainero, U. Costantino, M. Nocchetti, J.L.G. Fierro, J. Catal. 198 (2001) 338.
[19] F.J. Marino, E.G. Cerrella, S. Duhalde, M. Jobbagy, M.A. Laborde, Int. J. Hydrogen Energy 23 (1998) 1095.
[20] Y.-J. Tu, Y.-W. Chen, L. Chiuping, J. Mol. Catal. 89 (1994) 179–190.
[21] F. Severino, J.L. Brito, J. Laine, J.L.G. Fierro, A. Lopez Agudo, J. Catal. 177 (1998) 82.
[22] R.O. Idem, N.N. Bakhshi, Ind. Eng. Chem. Res. 34 (1995) 1548.
[23] I.E. Wachs, R.J. Madix, J. Catal. 53 (1978) 208.
[24] I.A. Fisher, A.T. Bell, J. Catal. 184 (1999) 357.
[25] R.G. Herman, K. Klier, G.W. Simmons, B.P. Finn, J.B. Bulko, J. Catal. 56 (1979) 407.
[26] J.E. Washs, R.J. Madix, J. Catal. 53 (1978) 208.
[27] R.J. Madix, Catal. Rev. Sci. Eng. 26 (1984) 281.